17 December 1999

ELSEVIER

Chemical Physics Letters 315 (1999) 25–30

CHEMICAL PHYSICS LETTERS

www.elsevier.nl/locate/cplett

Model of carbon nanotube growth through chemical vapor deposition

S.B. Sinnott [a,*], R. Andrews [a,b], D. Qian [a], A.M. Rao [b,c], Z. Mao [a], E.C. Dickey [a], F. Derbyshire [a,b]

[a] *Department of Chemical and Materials Engineering, University of Kentucky, Lexington, KY 40506, USA*
[b] *The Center for Applied Energy Research, University of Kentucky, Lexington, KY 40506, USA*
[c] *Department of Physics and Astronomy, University of Kentucky, Lexington, KY 40506, USA*

Received 14 July 1999; in final form 6 October 1999

Abstract

This Letter outlines a model to account for the catalyzed growth of nanotubes by chemical vapor deposition. It proposes that their formation and growth is an extension of other known processes in which graphitic structures form over metal surfaces at moderate temperatures through the decomposition of organic precursors. Importantly, the model also states that the form of carbon produced depends on the physical dimensions of the catalyzed reactions. Experimental data are presented that correlate nanotube diameters to the size of the catalyst particles. Nanotube stability as a function of nanotube type, length and diameter are also investigated through theoretical calculations.

Nanotubes have attracted much interest since their discovery in 1991 [1] because of their high modulus in the direction of the nanotube axis, electrical conductivity that could render them useful as nanometer-scale wires, and hollow structures that could be exploited in tailored membranes and molecular sieves [2]. Since their initial discovery, researchers have made tremendous progress in learning to synthesize carbon nanotubes in gram quantities. Nanotubes can be synthesized using arc-discharge [1], laser vaporization [3], or catalytic decomposition of hydrocarbons [4]. By adding the appropriate metal catalyst single-walled nanotubes (SWNTs) can be preferentially grown [5,6] while under other conditions multi-walled nanotubes (MWNTs) are grown almost exclusively [1]. While this progress is encouraging, there is still much that is not known about the growth mechanisms of nanotubes, something several research groups are attempting to better understand [7–13].

This Letter proposes a model to account for the growth of carbon nanotubes by catalytic decomposition of hydrocarbons (often termed chemical vapor deposition or CVD). The model sheds light on the way in which the reaction conditions influence the diameter and number of walls of the nanotubes. It is based on new experimental results, theoretical calculations, and data that have been published in the literature.

It is postulated that the formation and growth of nanotubes is an extension of other known processes in which graphitic structures are formed over metal

* Corresponding author. Tel.: +1-606-257-5857; fax: +1-606-323-1929; e-mail: sinnott@engr.uky.edu

0009-2614/99/$ - see front matter
PII: S0009-2614(99)01216-6

surfaces at temperatures below about 1100°C from carbon that is produced by the decomposition of a carbon-containing precursor. It is also proposed that the form of graphite that is produced is closely related to the physical dimensions of the metal catalyst particles. This hypothesis builds on a considerable volume of research that has been conducted over the past two to three decades on the formation of graphitic carbon over metal substrates [14,15]. The most effective metals have been shown repeatedly to be iron, nickel and cobalt [16]. The peculiar ability of these metals to form ordered carbons is thought to be related to a combination of factors. These include their catalytic activity for the decomposition of volatile carbon compounds, the fact that they form metastable carbides, and that carbon is able to diffuse through and over the metals extremely rapidly [14–16]. The latter property allows ordered carbon to be produced by a mechanism of diffusion and precipitation. This also means that graphitic structures are only formed in proximity to the metal surface. If there is significant reaction away from the metal, other undesirable forms of carbon, such as amorphous carbon nanoparticles, will be co-produced. Restriction of the reaction to the surface is controlled through the choice of the carbon precursor, its partial pressure and the reaction temperature.

Over thin metal foils, which in the present context can be considered as bulk metal, carbon dissolves to form a solid solution [16]. On cooling, it precipitates on the surface as a continuous thin film of highly crystalline graphite in which the graphite basal planes are oriented parallel to the substrate. The high degree of crystalline perfection that is obtained in a matter of seconds demonstrates that carbon atoms are extremely mobile and can move easily over and through the metal.

When the metal is present as particles of diameter in the range of tenths of a micron, the carbon is produced as filaments of similar diameter [14,15]. The metal particles can be supported on a substrate or introduced as 'floating' particles in a gas stream that flows through the reactor [17,18]. If the particles are considered to be spherical or pear shaped, the deposition of carbon atoms takes place on one half of the surface (on the lower curvature face for pear shapes). The carbon diffuses along the concentration gradient and precipitates on the opposite half, around and below the bisecting diameter. However, it does not precipitate from the apex of the hemisphere, which accounts for the hollow core that is characteristic of these filaments.

In the filament structure, the graphite crystallites precipitate with the basal plane tangential to the curved surface (as opposed to parallel to the surface for metal substrates with much larger dimensions). In cross-section, the filaments are composed of a series of crystallites whose ⟨c⟩ axis tends to follow the radial vector of the filament and whose basal planes follow the circumference, approximating the curved surface of the filament. The ⟨c⟩ axis may also be tilted at an angle to the radial vector, giving rise to a 'chevron' type structure. For supported metals, filaments can form either by 'extrusion' in which the fiber grows upwards from metal particles that remain attached to the substrate, or the particles detach and move at the head of the growing fibers, labeled 'tip-growth'. These mechanisms are illustrated graphically in Fig. 1 (after Baker and Harris [14]).

We have suggested [19] that the catalyst particle size determines the size of the 'filament'. As the particle diameter is reduced, the filament curvature increases, imposing an increasing strain on the basal planes of the crystallites. Eventually, a continuous surface is energetically more favorable and MWNTs are formed. Logically, if the particle size is reduced still further, SWNTs will be formed. The rest of this Letter outlines the experimental and theoretical evidence to support these arguments and hypotheses.

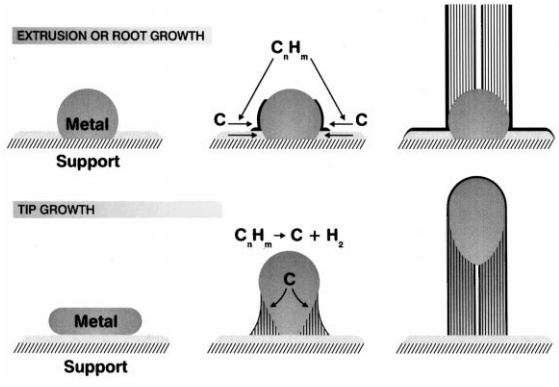

Fig. 1. Schematics of tip-growth and extrusion mechanisms for carbon filament growth (after Baker and Harris [14]).

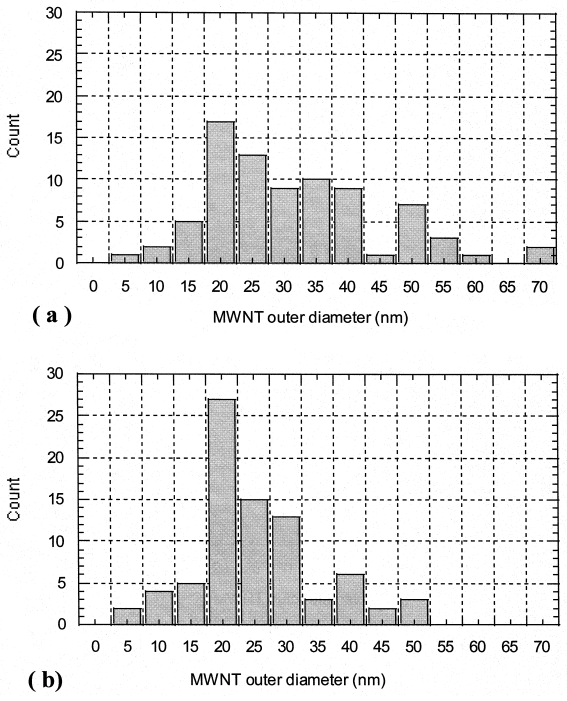

Fig. 2. Diameter distributions for MWNTs produced by chemical vapor deposition under (a) 0.75 at% Fe:C and (b) 0.075 at% Fe:C ratios.

In our experiments, aligned MWNTs were produced at high selectivity by the catalytic decomposition of a hydrocarbon feedstock, as described in detail elsewhere [19,20]. Briefly, about 6.5 mol% of ferrocene was dissolved in xylene and fed continuously into a two-stage quartz tube reactor. The liquid feed mixture was passed through a capillary tube and preheated to $\sim 175^{\circ}C$ prior to its entry into the furnace. At this temperature, liquid exiting the capillary is immediately volatilized and swept into the reaction zone of the furnace by a flow of argon with 10% hydrogen. Various parameters, such as the furnace temperature, ferrocene to xylene ratio, feed rate, reaction time, and sweep gas flow rate were adjusted to obtain growth conditions for high purity aligned MWNTs [19]. Carbon nanotube deposits were formed on the walls of the quartz furnace tube and on plain quartz substrates placed within the furnace.

Nanotubes were grown at two Fe:C atomic ratios, 0.75 and 0.075 at%. At the higher ratio, nanotubes were formed with an average diameter of about 33 nm and a diameter distribution as shown in Fig. 2a. The lower Fe:C ratio produced nanotubes with a smaller average diameter of about 28 nm and a noticeably narrower diameter distribution (Fig. 2b).

The data in Table 1 shows that the smaller average nanotube diameter obtained at the lower Fe:C ratio is directly related to the generation of smaller iron clusters. Under these conditions, a lower iron concentration in the vapor phase will limit the ability of the iron atoms to agglomerate into large clusters (giving larger nanotube diameters), leading to the formation of smaller iron clusters on the quartz substrate. It may be further supposed that the properties and temperature of the substrate will also influence the iron particle size. The selection of a substrate on which the metal is more mobile, and/or increasing the substrate temperature, will enhance the processes of nucleation and growth. This will lead to the formation of larger size particles and hence larger diameter nanotubes [19], ultimately affecting a transition to the growth of filaments rather than MWNTs. These suppositions will be examined in a continuing experimental program.

Table 1
Analytical results of as-grown MWNT samples

Fe/C (at%)	Average nanotube inner diameter (nm)	Average nanotube outer diameter (nm)	Average Fe particle diameter (nm)
0.75	5.8 (3.0)	33.6 (13.5)	35.3 (12.6)
0.075	4.3 (2.3)	28.3 (9.9)	28.2 (12.9)

The reactor was operated for 2 h at 675°C, with 20 mbar partial pressure of xylene and gas flows of 675 SCCM Ar and 75 SCCM H_2. Nanotube lengths were determined from images obtained using a scanning electron microscope (Hitachi, 3200N, 5 kV), while nanotube and Fe particle diameters were determined from images obtained using a transmission electron microscope (Hitachi, H-800 NA, 200 kV). The average nanotube and Fe particle diameters were obtained by fitting the raw data to a Gaussian normal distribution function. The data in parentheses are the standard deviations.

Transmission electron microscope images of the nanotubes formed at the two Fe:C ratios are shown in Fig. 3. The metal particles appear at the ends of the MWNTs and are of similar diameter to the nanotube, which supports the tip-growth (detached particle) model. The tip growth mechanism is further supported by the fact that once the nanotubes are detached from the quartz with a razor blade, the nanotube root ends appear to be open. However, it should be pointed out that the open ends could also be due to the ends being sheared off during their removal from the substrate. It is also possible that the nanotubes are directly attached to the substrate and do not possess the normal hemispherical end cap. Thus the growth mechanism is equivalent to that known for carbon filaments in which the nanotube or

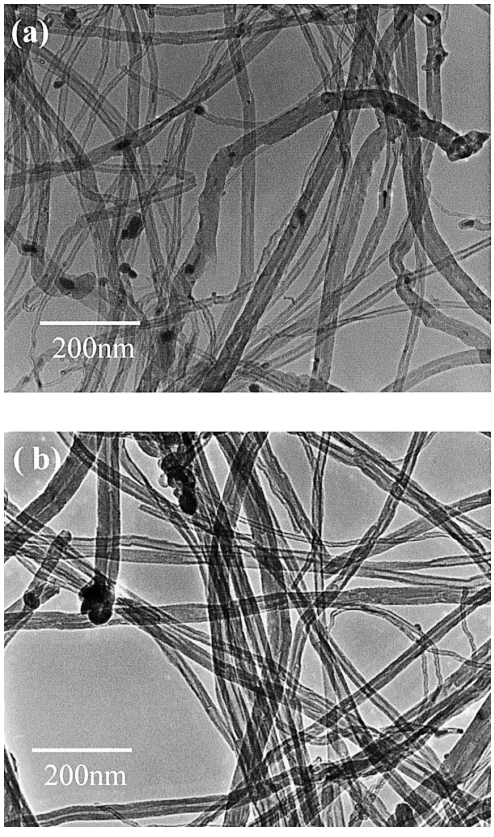

Fig. 3. Images from a transmission electron microscope (Hitachi, H-800 NA, 200 kV) of as-grown MWNTs with Fe catalyst particles at the tube ends. a) 0.75 at% Fe:C and b) 0.075 at% Fe:C ratios.

filament diameter relates to the metal particle size (where the limit is thought to be around 1 nm diameter for the SWNTs) and it also accounts for the hollow core in both structures.

Theoretical calculations were used to shed light on the relative stability of SWNTs, MWNTs and graphene as a function of size. The reactive empirical bond-order (REBO) potential developed by Tersoff [21] and parameterized for carbon and hydrogen by Brenner [22,23] is used in the calculations that consists of two-body and many-body terms. A long-range Lennard–Jones potential [24] is included that is only non-zero after the short-range covalent potential goes to zero. The REBO potential accurately models the energies, bond lengths, and lattice constants of both solid-state and molecular carbon materials, a crucial condition for the calculations presented below. It has therefore been used frequently to study carbon nanotubes [9,12,25–29]. However, like most empirical potentials the electrons are not treated explicitly so forces arising from effects such as orbital resonances and symmetry that could influence the stability of small structures are not addressed. However, it is used here because the size of some of the systems under considerations is prohibitively large ($\sim 10\,000$ atoms) for the use of more accurate quantum-mechanics-based methods.

It should be emphasized that the REBO potential cannot model carbon–metal interactions, so only pure carbon systems are examined in the calculations. The goal is to determine the most stable configuration of carbon for a limited size, defined as the number of atoms in the system. It is proposed that in the experiments this limited size would come about through a combination of reaction conditions and the size and shape of the metal catalyst particles.

The calculations confirm the trends discussed above of graphitic carbon structures having varying stability as a function of size. Fig. 4 shows the energy of a graphene sheet and (10,0), (19,0), (5,5) and (10,10) SWNTs as a function of the number of atoms in each system. For systems smaller than about 400 atoms, the (5,5) and (10,0) nanotubes, those with the smallest diameter, are the most stable (see the inset in Fig. 4). This is because the smaller nanotubes are longer and thus have a smaller percentage of edge atoms than the larger nanotubes. Above about 1000 atoms, the (10,10) and (19,0)

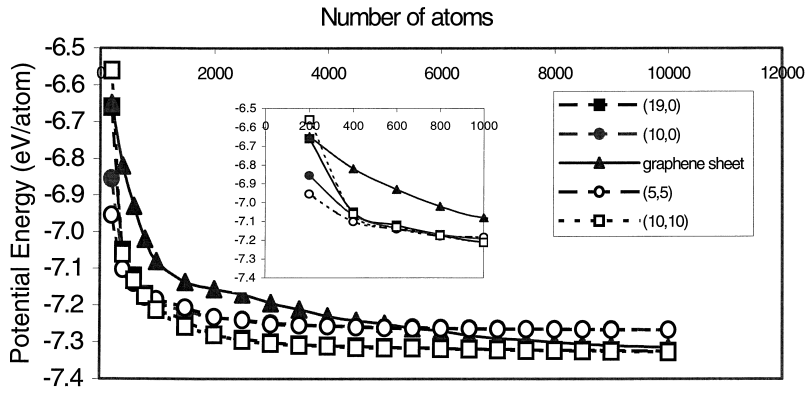

Fig. 4. Potential energy of (10,0), (19,0), (5,5) and (10,10) SWNTs and a graphene sheet as a function of number of atoms in each system.

nanotubes are preferred due to their lower strain. Fig. 4 also shows that nanotube stability depends on the diameter rather than on the helical symmetry in agreement with previous theoretical studies [30].

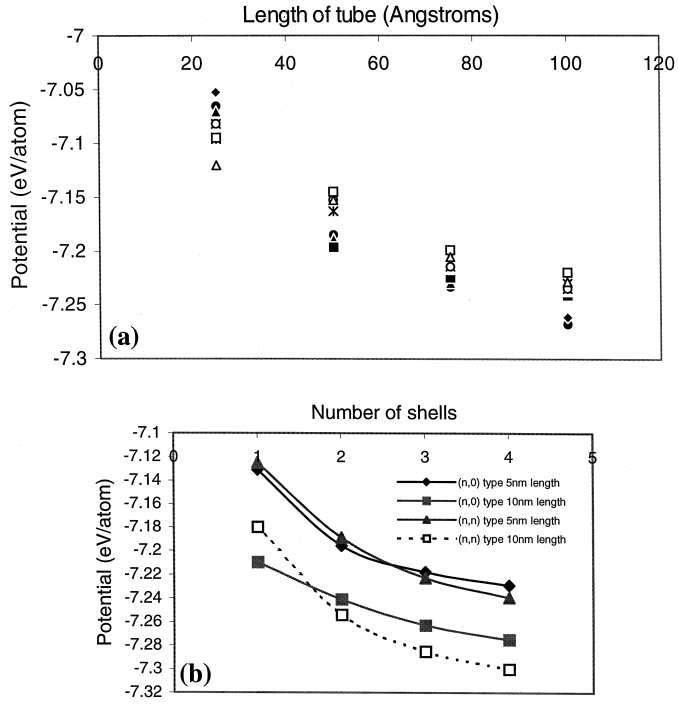

Fig. 5. (a) Potential energy of several MWNTs and SWNTs. ● is a MWNT of a (10,0) nanotube within a (12,12) nanotube, ♦ is a MWNT of a (5,5) nanotube within a (17,0) nanotube, ▲ is a MWNT of a (5,5) nanotube within a (10,10) nanotube, ■ is a (10,0) nanotube within a (19,0) nanotube, × is a (10,0) SWNT, * is a (19,0) SWNT, □ is a (5,5) SWNT, ○ is a (10,10) SWNT, and △ is a (12,12) SWNT. b) Potential energy of several MWNTs as a function of the number of shells in the nanotube. The shells in the MWNTs of (n,0) type are (10,0), (19,0), (29,0), and (39,0). The shells in the MWNTs of (n,n) type are (5,5), (10,10), (15,15), and (20,20).

The graphene is the least stable structure until about 6000 atoms where it becomes more stable than the (10,0) and (5,5) nanotubes. At the smaller sizes, the instability caused by the dangling bonds in the graphene is greater than the instability in the nanotubes due to strain. As the number of atoms continues to increase, the fraction of edge atoms in the graphene decreases, which continues to stabilize the graphene relative to the nanotubes.

Comparing the stability of SWNTs and MWNTs in Fig. 5a, we see that double-shell MWNTs become more stable as the number of atoms increase when compared to SWNTs on their own. This is because the Van der Waals interactions between the shells in the MWNT increase as the nanotube gets longer. A comparison is also made of the stability of different types of MWNTs, those where the helical arrangement of atoms in both shells are the same and those where they are different. Fig. 5a shows that there is little difference in the stability of MWNTs as a function of the helical arrangements of the shells. Fig. 5b illustrates how for a given nanotube length, as the number of shells goes up, the stability of the system increases, again due to an increase in the Van der Waals bonds between the nanotubes. Only small energy differences are seen between the MWNTs with different helical structures in their shells, with the differences becoming more significant at longer nanotube lengths.

Thus the calculations show that for systems constrained to a small number of atoms, SWNTs with small diameters are preferred. As the system size increases, SWNTs with larger diameters become more stable followed by MWNTs. As the system size increases further, MWNTs with a higher number of shells become increasingly preferred. The experimental evidence shows that in the growth of carbon species over metal catalyst particles under identical conditions (see Table 1), smaller MWNTs are grown preferentially in narrower diameter distributions when the catalyst particle sizes are smaller. Taken together with the tip-growth and extrusion mechanisms, that are well-understood for the growth of filamentous carbon fibers, these results bring us closer to achieving structural control over nanotubes synthesized via chemical vapor deposition.

Acknowledgements

This work was supported by a National Science Foundation MRSEC (DMR-9809686). Z.M. and S.B.S. also acknowledge support from the NASA-Ames Research Center (NAG 20-1121).

References

[1] S. Iijima, Nature 354 (1991) 56.
[2] M.S. Dresselhaus, G. Dresselhaus, P.C. Eklund, Science of Fullerenes and Carbon Nanotubules, Academic Press, San Diego, 1996.
[3] T. Guo et al., Chem. Phys. Lett. 243 (1995) 49.
[4] W.Z. Li et al., Science 274 (1996) 1701.
[5] D.S. Bethune et al., Nature 363 (1993) 605.
[6] S. Iijima, T. Ichihashi, Nature 363 (1993) 603.
[7] Y.H. Lee, S.G. Kim, D. Tomanek, Phys. Rev. Lett. 78 (1997) 2393.
[8] Y.-K. Kwon et al., Phys. Rev. Lett. 79 (1997) 2065.
[9] C.F. Cornwell, L.T. Wille, J. Chem. Phys. 109 (1998) 763.
[10] C.-H. Kiang, W.A. Goddard III, Phys. Rev. Lett. 76 (1996) 2515.
[11] M.B. Nardelli et al., Phys. Rev. Lett. 80 (1998) 313.
[12] A. Maiti, C.J. Brabec, J. Bernholc, Phys. Rev. B 55 (1997) R6097.
[13] S. Fan et al., Science 283 (1999) 512.
[14] R.T.K. Baker, P.S. Harris, Formation of Filamentous Carbon in Chemistry and Physics of Carbon 14, Marcel Dekker, New York, 1978, p. 83.
[15] R.T.K. Baker, Carbon 27 (1989) 315.
[16] F.J. Derbyshire, A.E.B. Presland, D.L. Trimm, Carbon 13 (1975) 111.
[17] M. Endo et al., Proc. of the NATO-Advanced Study Institute, Antalaya, Turkey, 1998.
[18] C.H. Kiang et al., Phys. Rev. Lett. 81 (1998) 1869.
[19] R. Andrews et al., Chem. Phys. Lett. 303 (1999) 467.
[20] D. Jacques et al., Chem. Phys. Lett., in preparation.
[21] J. Tersoff, Phys. Rev. B 39 (1989) 5566.
[22] D.W. Brenner, S.B. Sinnott, O.A. Shenderova, J.A. Harrison, unpublished.
[23] D.W. Brenner, Phys. Rev. B 42 (1990) 9458.
[24] J.-P. Ryckaert, A. Bellemans, Chem. Phys. Lett. 30 (1975) 123.
[25] S.B. Sinnott et al., Carbon 36 (1998) 1.
[26] B.I. Yakobson et al., Comp. Mater. Sci. 8 (1997) 341.
[27] B.I. Yakobson, C.J. Brabec, J. Bernholc, Phys. Rev. Lett. 76 (1996) 2511.
[28] J.A. Harrison et al., J. Phys. Chem. B 101 (1997) 9682.
[29] A. Garg, S.B. Sinnott, Chem. Phys. Lett. 295 (1998) 273.
[30] D.H. Robertson, D.W. Brenner, J.W. Mintmire, Phys. Rev. B 45 (1992) 12592.